



Mallalieu, Joseph ORCID logoORCID: <https://orcid.org/0000-0002-1988-8594>, Carrivick, Jonathan, Quincey, Duncan and Raby, Cassandra (2021) Ice-marginal lakes associated with enhanced recession of the Greenland Ice Sheet. *Global and Planetary Change*, 202. pp. 1-12.

Downloaded from: <https://ray.yorks.ac.uk/id/eprint/5240/>

The version presented here may differ from the published version or version of record. If you intend to cite from the work you are advised to consult the publisher's version:
<https://www.journals.elsevier.com/global-and-planetary-change>

Research at York St John (RaY) is an institutional repository. It supports the principles of open access by making the research outputs of the University available in digital form. Copyright of the items stored in RaY reside with the authors and/or other copyright owners. Users may access full text items free of charge, and may download a copy for private study or non-commercial research. For further reuse terms, see licence terms governing individual outputs. [Institutional Repositories Policy Statement](#)

RaY

Research at the University of York St John

For more information please contact RaY at
ray@yorks.ac.uk

Ice-marginal lakes associated with enhanced recession of the Greenland Ice Sheet

Joseph Mallalieu^{a,b,*}, Jonathan L. Carrivick^b, Duncan J. Quincey^b, Cassandra L. Raby^c

^aSchool of Humanities, York St John University, York, YO31 7EX, UK

^bSchool of Geography and water@leeds, University of Leeds, Leeds, LS2 9JT, UK

^cInstitute of Integrative Biology, University of Liverpool, Liverpool, L69 7ZB, UK

*Corresponding author: j.mallalieu@yorks.j.ac.uk

HIGHLIGHTS

- Prevalent and accelerating ice-margin recession in south-west Greenland from 1992
- Contrasting ice-marginal environments demonstrate a heterogeneous response to warming
- Lacustrine ice-margins recede faster than terrestrial, but slower than marine margins
- Lacustrine recession rates progressively outpaced terrestrial rates between 1987-2015
- Significant correlations between lake parameters and recession rates are identified

ABSTRACT

There has been a progressive increase in the number and area of ice-marginal lakes situated along the south-western margin of the Greenland Ice Sheet (GrIS) since the 1980s. The increased prevalence of ice-marginal lakes is notable because of their capacity to enhance mass loss and ice-margin recession through a number of thermo-mechanical controls. Although such effects have been extensively documented at alpine glaciers, an understanding of how ice-marginal lakes impact the dynamics of

the GrIS has been limited by a sparsity of observational records. This study employs the Landsat archive to conduct a multi-decadal, regional-scale statistical analysis of ice-margin advance and recession along a ~5000 km length of the south-western margin of the GrIS, incorporating its terrestrial, lacustrine and marine ice-margins. We reveal an extended and accelerating phase of ice-margin recession in south-west Greenland from 1992 onwards, irrespective of margin type, but also observe considerable heterogeneity in the behaviour of the different ice-marginal environments. Marine ice-margins exhibited the greatest magnitude and variability in ice-margin change, however lacustrine termini were notable for a progressive increase in ice-margin recession rates from 1987 to 2015, which increasingly outpaced those measured at terrestrial ice-margins. Furthermore, significant correlations were identified between lake parameters and rates of lacustrine ice-margin recession, including lake area, latitude, altitude and the length of the lake – ice-margin interface. These results suggest that ice-marginal lakes have become increasingly important drivers of ice-margin recession and thus mass loss at the GrIS, however further research is needed to better parameterise the causal connections between ice-marginal lake evolution and enhanced ice-margin recession. More widely, a detailed understanding of the impacts of ice-marginal lakes on ice-margin dynamics across Greenland is increasingly necessary to accurately forecast the response of the ice sheet to enhanced ice-marginal lake prevalence and thus refine projections of recession, mass loss and sea level rise.

KEYWORDS: Greenland Ice Sheet; ice-marginal lake; proglacial lake; glacier dynamics; meltwater

1. INTRODUCTION

Since a period of near equilibrium mass balance in the 1980s, rates of mass loss at the Greenland Ice Sheet (GrIS) have generally accelerated in response to increased atmospheric and oceanic warming (Hanna et al., 2013; Shepherd et al., 2020). Over the same time period, enhanced rates of meltwater runoff (Hanna et al., 2008; Trusel et al., 2018) have coincided with a progressive increase in the number and area of ice-marginal lakes situated along the south-western margin of the GrIS (Carrivick

and Quincey, 2014; How et al. 2021). The presence of ice-marginal lakes is significant because of their capacity to regulate ice-margin dynamics through a number of thermo-mechanical controls, including the onset and promotion of calving (Carrivick and Tweed, 2013). In particular, ice-marginal lake formation and expansion is typically associated with enhanced rates of mass loss and ice-margin recession (e.g. Kirkbride, 1993; Boyce et al., 2007; Schomacker, 2010; Basnett et al., 2013; Brun et al., 2019; King et al., 2019; Tsutaki et al., 2019; Liu et al., 2020; Sutherland et al., 2020). However, whilst the effects of ice-marginal lakes on alpine glacier dynamics have been increasingly well-documented, knowledge of their effects on the dynamics of ice sheets is presently limited by a sparsity of observational records (Mallalieu et al., 2017, 2020). A detailed understanding of the impacts of ice-marginal lakes on ice-margin dynamics across Greenland is therefore increasingly necessary to accurately forecast the response of the ice sheet to enhanced ice-marginal lake prevalence and thus further refine projections of mass loss and sea level rise.

An analysis of outlet glacier extent by Warren (1991) revealed significant variability in the behaviour of the terrestrial, lacustrine and marine outlets of the GrIS throughout the mid-20th century, despite having undergone comparable climatic forcing. Both lacustrine and marine outlets were found to exhibit much greater variability in frontal behaviour than their terrestrial counterparts due to their partial decoupling from climatic forcing and the increased role of topographic and bathymetric controls on terminus advance and recession. However, subsequent analyses of ice-margin behaviour and extent in Greenland have omitted measurements from lacustrine ice-margins, instead focusing on changes at the major marine-terminating outlets (e.g. Howat et al., 2008; Howat and Eddy, 2011; Catania et al., 2018), and the terrestrial termini of peripheral glaciers and ice caps (PGICs) (e.g. Citterio et al., 2009; Leclercq et al., 2012; Rastner et al., 2012; Bjørk et al., 2018). In addition, the few studies that have incorporated measurements of ice-margin change from terrestrial outlets of the main ice sheet typically include a sparse number of terrestrial data points (e.g. Moon and Joughin, 2008; Carr et al., 2013; Mouginot et al., 2019), or concern a relatively limited footprint in south-east Greenland

(e.g. Kargel et al., 2012; Mernild et al., 2012). As a consequence, the relative magnitude of recent changes at the terrestrial, lacustrine and marine margins of the GrIS remain unknown.

The long temporal record of the Landsat image archive, now extending into its fourth decade with the launch of Landsat 8 (Roy et al., 2014), provides a unique opportunity to perform a multi-decadal, regional-scale analysis of ice-margin extent for the disparate ice-marginal environments of the GrIS between the 1980s and the present day. South-west Greenland is the optimal site for such an analysis because: (i) it has the greatest regional concentration of land-terminating, and thus lacustrine, margins of the GrIS (Figure 1); (ii) the region has experienced some of the highest increases in mean annual air temperatures recorded in the Arctic since the 1990s (Carr et al., 2013; Ding et al., 2014); and (iii) the region is forecast to undergo some of the greatest rates of ice-margin recession and reductions in ice-cover over the next millennium (Aschwanden et al., 2019).

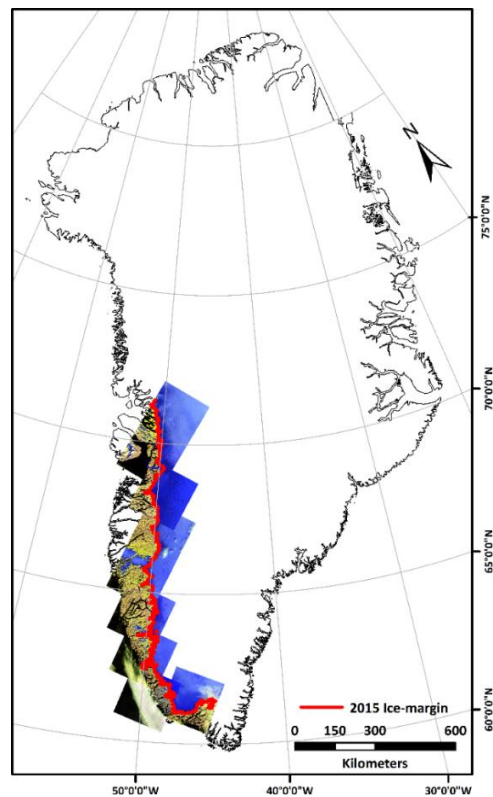


Figure 1. Study location in south-west Greenland. The spatial extent of the analysis is illustrated with false-colour Landsat scenes from 2015 (see Table 1).

95 [SINGLE COLUMN WIDTH]

96 Table 1. Attributes of Landsat scenes used in this study.

Epoch	Sensor	Scene ID	Date of acquisition	Path	Row
2015	OLI	LC80010172015227LGN00	15/08/2015	1	17
	OLI	LC80020172015234LGN00	22/08/2015	2	17
	OLI	LC80040172015216LGN00	04/08/2015	4	17
	OLI	LC80050162015255LGN00	12/09/2015	5	16
	OLI	LC80060152015214LGN00	02/08/2015	6	15
	OLI	LC80060162015214LGN01	02/08/2015	6	16
	OLI	LC80070132015237LGN00	25/08/2015	7	13
	OLI	LC80070142015237LGN00	25/08/2015	7	14
	OLI	LC80080122015196LGN00	15/07/2015	8	12
	OLI	LC80100102015210LGN00	29/07/2015	10	10
	OLI	LC80100112015210LGN00	29/07/2015	10	11
2010	ETM+	LE70020172011231EDC00	19/08/2011	2	17
	ETM+	LE70040162009207EDC00	26/07/2009	4	16
	ETM+	LE70040172009207EDC00	26/07/2009	4	17
	ETM+	LE70060152011211ASN00	30/07/2011	6	15
	ETM+	LE70070132010231EDC00	19/08/2010	7	13
	ETM+	LE70070142011234EDC00	22/08/2011	7	14
	ETM+	LE70090112009210EDC00	29/07/2009	9	11
	ETM+	LE70090122010229EDC00	17/08/2010	9	12
	ETM+	LE70100102009217ASN00	05/08/2009	10	10
2005	ETM+	LE70020172004244ASN01	31/08/2004	2	17
	ETM+	LE70040162007202EDC00	21/07/2007	4	16
	ETM+	LE70040172007202EDC00	21/07/2007	4	17
	ETM+	LE70060142007216EDC00	04/08/2007	6	14
	ETM+	LE70060152006245EDC00	02/09/2006	6	15
	ETM+	LE70070132005217EDC00	05/08/2005	7	13
	ETM+	LE70090112007221EDC00	09/08/2007	9	11
	ETM+	LE70090122007221EDC00	09/08/2007	9	12
	ETM+	LE70110102005229EDC00	17/08/2005	11	10
2000	ETM+	LE70020172000217AGS00	04/08/2000	2	17
	ETM+	LE70040161999212EDC01	31/07/1999	4	16
	ETM+	LE70040171999212EDC01	31/07/1999	4	17
	ETM+	LE70060152001215AGS00	03/08/2001	6	15
	ETM+	LE70070132001190EDC00	09/07/2001	7	13
	ETM+	LE70070142001190EDC00	09/07/2001	7	14
	ETM+	LE70090112001188EDC00	07/07/2001	9	11
	ETM+	LE70090122001188EDC00	07/07/2001	9	12
	ETM+	LE70100102000257SGS00	13/09/2000	10	10
1992	ETM+	LE70110102000168EDC00	16/06/2000	11	10
	TM	LT50020171992219PAC00	06/08/1992	2	17
	TM	LT50040161992217PAC00	04/08/1992	4	16
	TM	LT50040171992217PAC00	04/08/1992	4	17
	TM	LT50050161993242PAC00	30/08/1993	5	16
	TM	LT50060141992263PAC00	19/09/1992	6	14
	TM	LT50060151992263PAC00	19/09/1992	6	15
	TM	LT50080121994170KIS00	19/06/1994	8	12
	TM	LT50080131994170PAC00	19/06/1994	8	13
1987	TM	LT40090111992212XXX02	30/07/1992	9	11
	TM	LT50050151987242XXX03	30/08/1987	5	15
	TM	LT50050161987258XXX01	15/09/1987	5	16
	TM	LT50060141987201XXX08	20/07/1987	6	14
	TM	LT50060151987201XXX08	20/07/1987	6	15
	TM	LT50070131987176XXX01	25/06/1987	7	13
	TM	LT40080121988146XXX01	25/05/1988	8	12
	TM	LT50090111985248KIS00	05/09/1985	9	11
	TM	LT40090121988169XXX01	17/06/1988	9	12
1987	TM	LT50110101987236KIS00	24/08/1987	11	10

97 [SINGLE COLUMN WIDTH]

This study therefore aims to quantify changes in ice-margin extent at the terrestrial, lacustrine and marine margins of the GrIS in south-west Greenland, and to investigate how the properties of ice-marginal lakes relate to rates of lacustrine ice-margin change. The objectives comprise: (i) the generation of an ice-marginal lake inventory and delineation of the ice sheet margin for 6 epochs at approximately 5-year intervals between 1987 and 2015; (ii) the quantification of ice-margin advance and recession at terrestrial, lacustrine and marine ice-margins between successive epochs; and (iii) a statistical analysis of ice-marginal lake parameters and rates of change at lacustrine margins.

2. DATA AND METHODS

2.1 LANDSAT SCENE SELECTION

A total of 58 Landsat Thematic Mapper (TM), Enhanced Thematic Mapper Plus (ETM+) and Operational Land Imager (OLI) scenes were downloaded from the USGS Global Visualisation Viewer to encompass the predominantly terrestrial margins of the GrIS in south-west Greenland between the mid-1980s and 2015 (Figure 1, Table 1). All scenes were Level 1TP (radiometrically calibrated and orthorectified) products and possessed a horizontal ground resolution of 30 m. The scenes were selected to coincide with the melt season (late May to early September) in order to minimise seasonal variability and to also reduce the incidence of frozen lakes and snow cover along the ice-margin. Extensive cloud and/or persistent snow cover in some years necessitated a flexible sampling interval for the acquisition of scenes throughout the study period. Therefore, following the method of Carrivick and Quincey (2014), scenes were assigned to one of 6 epochs (1987, 1992, 2000, 2005, 2010 and 2015), with 86 % of scenes acquired within ± 1 year of their respective epoch, and the remaining scenes acquired within ± 2 years (Table 1). Scenes in the 2005 and 2010 epochs were also selected to mitigate the effects of the failed ETM+ Scan Line Corrector (SLC) by utilising the considerable scene overlap within the study area. Where SLC failure induced stripes were unavoidable, gaps were filled via mosaicing with an unaffected

scene from the closest viable time period. Processing of the Landsat scenes was conducted in software ENVI v.5.2 and Esri ArcMap v.10.3.1.

2.2 ICE-MARGINAL LAKE INVENTORY

The ice-marginal lake inventory used in this study was derived by refining the 1987-2010 lake dataset mapped in Carrivick and Quincey (2014) and extending the duration of the survey to incorporate Landsat scenes from 2015. Details of the scene processing are fully described and evaluated in Carrivick and Quincey (2014), hence a synopsis is provided here. Scenes were classified by applying the Normalised Difference Water Index (NDWI) (McFeeters, 1996) to the near infrared (NIR) and blue bands of the respective TM, ETM+ and OLI spectral channels, where $NDWI = ((B_{NIR} - B_{Blue}) / (B_{NIR} + B_{Blue}))$ and B is the spectral channel. The blue, rather than the more established green, spectral channel was employed because of its improved ability to discriminate water from snow and ice in cold environments (Huggel et al., 2002). An upper NDWI threshold of -0.5 was used to automatically detect lakes and a median filter (3×3 kernel) was used to reduce noise and remove isolated pixels. Classified lakes were exported as polygons for quality assurance in ArcMap, with misclassified areas of cloud and shadow manually corrected through comparison with scenes from adjacent epochs. Manual digitisation was used to delineate several frozen lakes, accounting for ~0.5 % of the total lake dataset. The analysis here was subsequently restricted to lakes that: (i) retained contact with the ice-margin; (ii) were endorheic (with no visible outflow); and (iii) were greater than 25,000 m² in area. The ice-contact and endorheic conditions were included to specifically consider the effect of meltwater retention on ice-margin change.

In order to establish a dataset of lake parameters, each lake was assigned a consistent identifier throughout the study period by calculating the centroid of the total lake extent (the maximum outline of a given lake across all epochs) (Figure 2). Lake areas were subsequently calculated within each epoch, but lakes that lost ice-contact via drainage or ice-margin recession were discounted from the

dataset for the respective epoch(s). In the event of a partial lake drainage, only the lake basin that maintained ice-contact was retained in the analysis (e.g. Figure 3). In addition, each lake was assigned a persistence score (from 1-6) to indicate its permanence across the 6 epochs. The length of the interface between individual lakes and the ice-margin was measured by calculating the geometric intersection of lake polygons and the delineated ice-margin to within a tolerance of 30 m (Figure 3). Finally, the latitude and altitude of each lake centroid was extracted from a Digital Elevation Model (DEM) of the GrIS generated from 1985 aerial photography, with a ground resolution of 25 m and horizontal and vertical accuracies of ± 10 m ± 6 m respectively (Korsgaard et al., 2016). The delineation of lake extent was assumed to be accurate to within ± 1 pixel (30 m) of the true lake perimeter. Consequently, the absolute error associated with each area measurement was dependent on lake size and planform, and thus resulted in a declining power law relationship whereby the greatest errors were associated with the smallest lakes. For example, lakes measuring 0.5 km^2 had an area uncertainty of $\sim 9 \%$, whilst lakes measuring $> 5 \text{ km}^2$ had an uncertainty of $< 3 \%$.

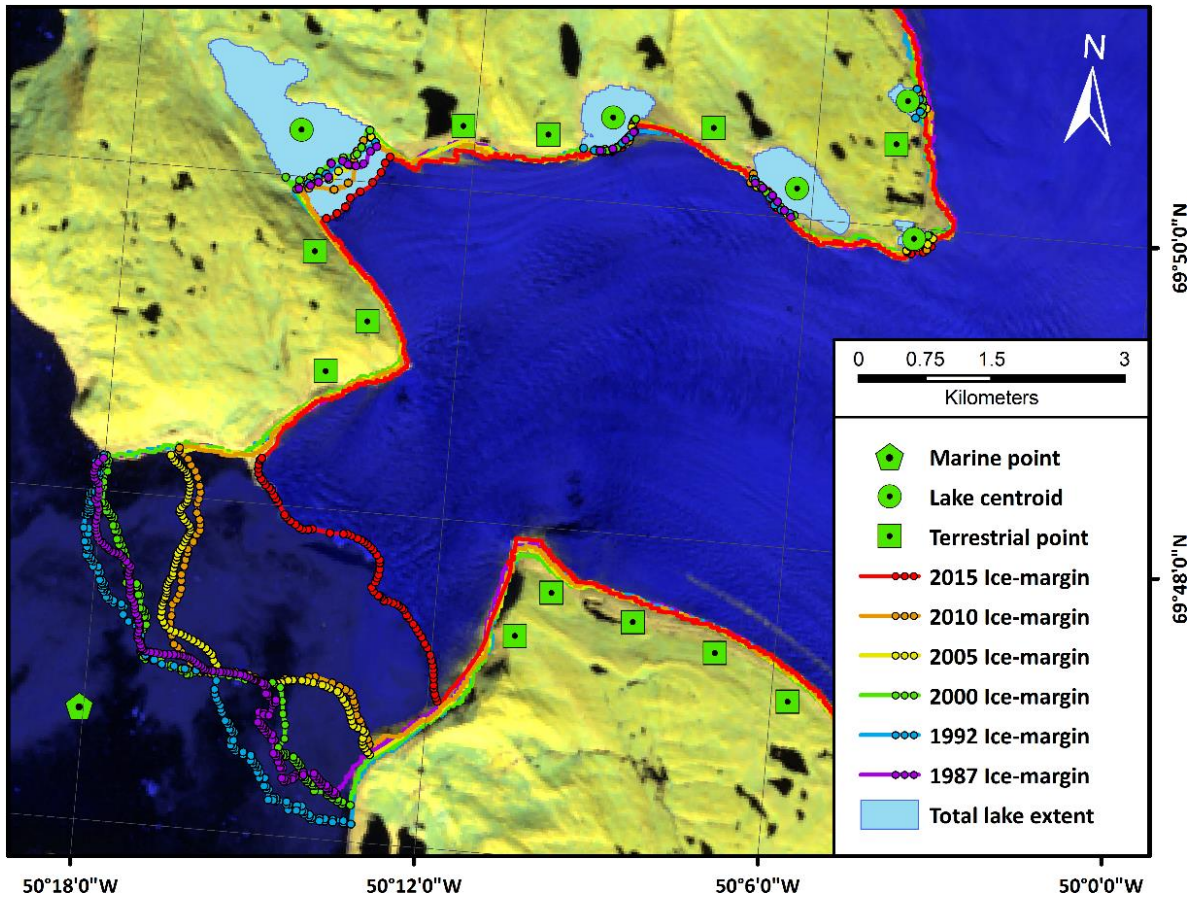
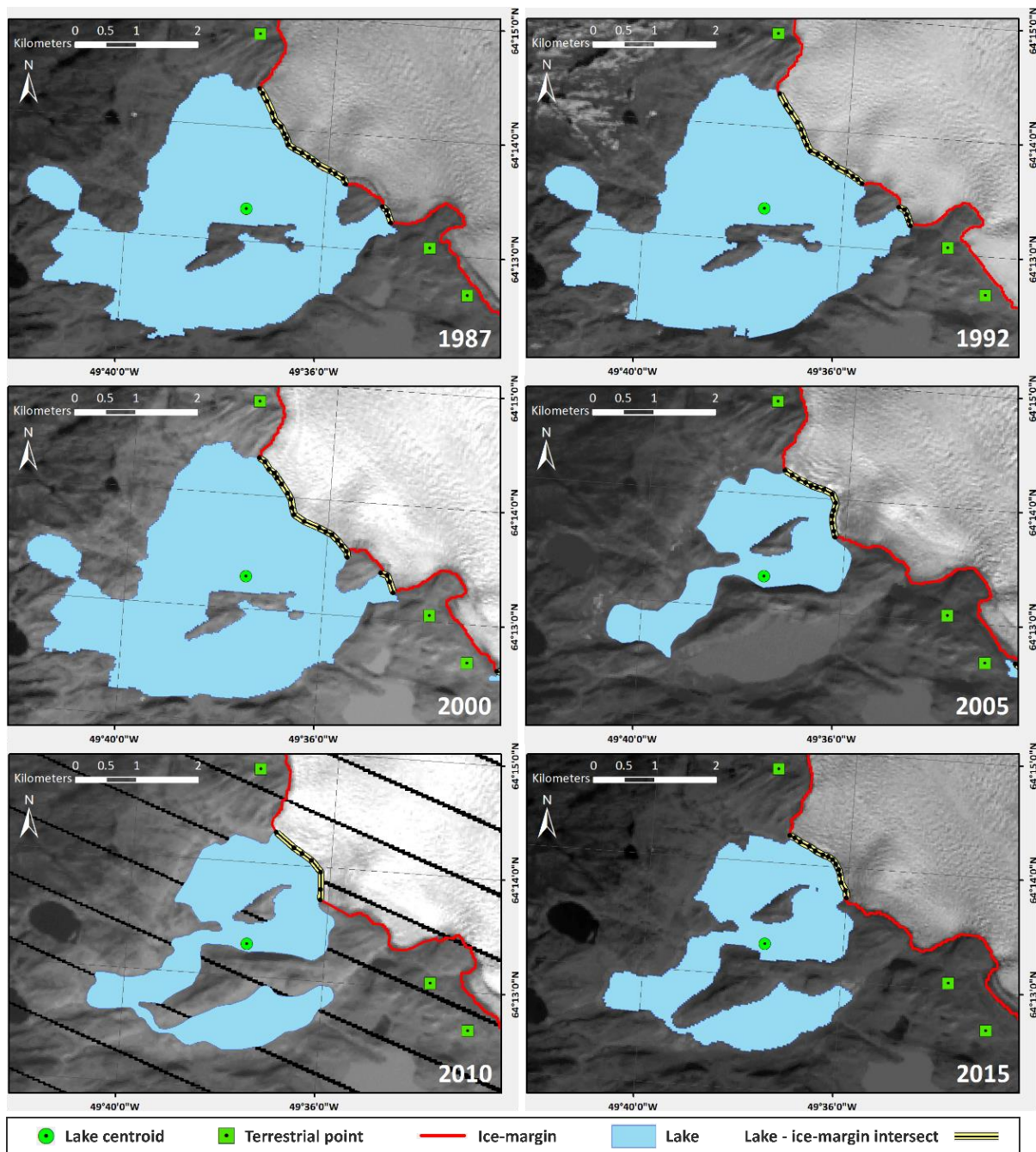


Figure 2. Example of dataset, comprising terrestrial, lacustrine and marine ice-margins, and the respective fixed points/centroids used for measurements of ice-margin change. Small circles on marine and lacustrine ice-margins represent the vertices over which distance measurements are averaged. Total lake extent represents the maximum outline of each lake across all epochs. Basemap: 2015 false-colour Landsat OLI scene.

[DOUBLE COLUMN WIDTH]

189
190



191

192 Figure 3. Example of temporal variation in lake area and lake – ice-margin intersect over the survey
193 period. In particular note the partial lake drainage between 2000 and 2005, and subsequent refilling.

194 [DOUBLE COLUMN WIDTH]

195

196 2.3 ICE-MARGIN DELINEATION

The ice sheet margin in south-west Greenland was delineated by using the green and shortwave infrared (SWIR) bands of the respective TM, ETM+ and OLI spectral channels to classify scenes with the Normalised Difference Snow Index (NDSI) (Hall et al., 1995), where $NDSI = \frac{(B_{Green} - B_{SWIR})}{(B_{Green} + B_{SWIR})}$. An NDSI threshold of 0.45 ± 0.1 was used to classify areas of snow and ice on a scene by scene basis with the aim of minimising subsequent manual post-processing. Due to the similar spectral properties of snow, ice and water in the green and SWIR spectral bands, an additional threshold of 0.45 was applied in the respective NIR band to mask out water bodies in the ice-marginal environment and thus improve the accuracy of ice-margin delineation. A median filter (3x3 kernel) was also applied to reduce noise and remove small snow patches. Manual editing was subsequently employed to refine the delineated ice-margins in isolated areas affected by shadow, debris cover and late-lying snow. Consistent mapping of the ice-margin was achieved in these regions through consultation with scenes from neighbouring epochs and high resolution DigitalGlobe imagery in Google Earth. Finally, delineated ice-margins in adjacent scenes were merged to generate a single ice-margin for south-west Greenland within each epoch (Figures 1, 3), which were subsequently used to derive the measurements of ice-margin advance and recession detailed in Section 2.4. Measurements of total ice-margin length, comparable to the length of the lake – ice-margin intersects detailed in Section 2.2, were generated by smoothing the delineated ice-margins to a tolerance of 30 m. Given that all results presented here are regionally aggregated, it is assumed that any over-estimation of the ice-margin position is cancelled out by an equal and opposite under-estimation, and uncertainty in the ice-margin positions is therefore not specifically assessed for these bulk figures.

2.4 MEASUREMENTS OF ICE-MARGIN CHANGE

Rates of ice-margin advance and recession between successive epochs were calculated by measuring changes in ice-margin position relative to a series of fixed reference points across the study period. Existing techniques for measuring changes in glacier extent have been primarily developed to quantify changes in the position of glacier termini occupying troughs (e.g. Lea et al., 2014), and are thus

unsuited to analysing changes at lacustrine margins which typically occupy a greater diversity of ice-marginal environments, particularly the lateral margins of outlet glaciers (cf. Figure 2). For example, techniques that measure change along the centre-line of the glacier (e.g. Bevan et al., 2012; Mernild et al., 2012) are not applicable at the majority of lacustrine margins. In addition, the highly dynamic nature of many lake – ice-margin interfaces (cf. Figure 3) prevents the use of fixed boxes to calculate area averaged advance or recession between successive epochs (e.g. Howat and Eddy, 2011; Hill et al., 2018). Therefore, changes in the extent of lacustrine and marine ice-margins here were measured using the bow method outlined in Bjørk et al. (2012). The centroids of the total lake extents were used as fixed reference points from which to measure distances to the respective lake – ice-margin intersect within each epoch, with a series of points established on the vertices of each intersect to permit the calculation of a mean lake centroid – intersect distance (Figure 2). Rates of ice-margin advance or recession were then calculated by differencing the mean distance values in successive epochs and dividing by the interval duration. Consequently, rates of change at lacustrine margins were only generated when a lake was present in two or more successive epochs. In the rare instances in which a lake – ice-margin intersect was manifest in multiple sections (e.g. Figure 3) the loss/addition of intersect sections between successive epochs resulted in small under- and over-estimates of ice-margin recession respectively, which collectively had a negligible effect on the aggregated measures of lacustrine margin change. Changes in the extent of marine margins were measured in the same manner as lacustrine margins by establishing fixed marine points in front of each terminus and calculating changes in mean distance between the marine points and respective marine margin vertices in successive epochs (Figure 2). Changes at terrestrial margins were calculated by creating a series of fixed points at 1 km intervals along a 250 m buffer of the delineated 1992 ice-margin. Distances between the fixed terrestrial points and the proximal point on the terrestrial margin were measured using proximity analysis and subsequently differenced to calculate rates of advance and recession between successive epochs.

2.5 STATISTICAL ANALYSES

Data were analysed using multivariate regression methods in R v.3.6.0 (R Core Team, 2019) to: (i) investigate differences in rates of change at terrestrial, lacustrine and marine ice-margins; and (ii) assess the influence of lake parameters on rates of change at lacustrine margins. Two linear mixed-effects models (LMMs) were fitted (Bates et al., 2015) using the rate of ice-margin change as the dependent variable in both models. One data point from Jakobshavn Isbrae was omitted due to its extreme outlying status (> 2 km recession between the 2000 and 2005 epochs). The repeated sampling of the same sites across epochs was accounted for by including location as a random effect. LMM 1 compared rates of change at the disparate margin types, and included: ice-margin type (lacustrine, marine, terrestrial); epoch; and latitude as independent variables (with latitudinal data included to control for the spatial clustering of particular margin types along the ice-margin). LMM 2 assessed rates of change at lacustrine margins, and included the independent variables: latitude; altitude; lake area; intersect length; persistence; and epoch. All independent variables were tested for multicollinearity prior to model fitting; however, lake area and intersect length failed to meet this assumption ($|r| > 0.7$; Dormann et al., 2013). Consequently, two alternate versions of LMM 2 were fitted to accommodate lake area and intersect length respectively.

3. RESULTS

3.1 MODEL FIT

Testing of the fitted LMMs for normality and heteroscedasticity revealed that the distribution of the residuals was heavy-tailed. Consequently, additional Robust LMMs were constructed to assess the impact of outliers on model fit (Koller, 2006). The resultant similarity of the respective LMM and Robust LMM coefficients (Table 2) indicated that the outliers had a limited effect on the fit of the models, therefore the outputs of the initial LMMs are presented henceforth.

Table 2. LMM and Robust LMM model variables and coefficients.

LMM 1*			LMM 2(a)			LMM 2(b)		
Ind. variables	LMM	Robust LMM	Ind. variables	LMM	Robust LMM	Ind. variables	LMM	Robust LMM
Epoch	-0.120	-0.081	Latitude	0.065	0.051	Latitude	0.068	0.049
Type:Marine	-2.637	-0.612	Altitude	0.132	0.074	Altitude	0.132	0.073
Type:Terrestrial	0.215	0.100	Lake area	-0.191	-0.074	Intersect length	-0.223	-0.095
Latitude	0.020	0.012	Epoch	-0.157	-0.142	Epoch	-0.153	-0.142
			Persistence	0.030	0.021	Persistence	0.094	0.049

* Note reference values for categorical variables 'Type' in LMM 1 are Lacustrine.

[DOUBLE COLUMN WIDTH]

3.2 ICE-MARGIN CHANGE AT TERRESTRIAL, LACUSTRINE AND MARINE MARGINS

The ice-margins mapped in this study delineate a ~5000 km length of the south-western margin of the GrIS. Cumulative totals of ice-margin type remained broadly consistent between 1987 and 2015, with ~89 % of the ice-margin in the study area terminating in a terrestrial setting, ~8 % in a lacustrine setting and ~3 % in a marine setting (Table 3). The number of measurements of ice-margin change between successive epochs was substantial throughout the study period, with each period incorporating measurements from between 22 to 35 marine margins, 353 to 439 lacustrine margins and 2469 to 3325 terrestrial margins (Table 4). From 1992 onwards, mean change at all margin types was negative, signifying an extended duration of ice-margin recession in south-west Greenland. However, positive values of mean change between 1987 and 1992 reveal an earlier period of ice-margin advance at both terrestrial and marine margins, although mean change at lacustrine margins remained negative (Table 4).

Table 3. Summary statistics of ice-margin composition in south-west Greenland throughout the study period.

Epoch	Total ice-margin length		Terrestrial ice-margin length		Lacustrine ice-margin length		Marine ice-margin length	
	km	% of total	km	% of total	km	% of total	km	% of total
1987	3722*	100.00	3306	88.82	319	8.56	98	2.63
1992	5029	100.00	4500	89.47	398	7.91	132	2.62
2000	5019	100.00	4466	88.98	421	8.38	132	2.64
2005	4916	100.00	4377	89.04	405	8.24	133	2.71
2010	4966	100.00	4429	89.19	402	8.10	135	2.71
2015	4932	100.00	4345	88.10	434	8.80	153	3.10

* The reduced length of the 1987 ice-margin is due to the unavailability of Landsat TM scenes from the southern end of the study area in the years 1985-1988.

[DOUBLE COLUMN WIDTH]

Table 4. Summary statistics of ice-margin change in south-west Greenland throughout the study period. Note positive and negative values represent ice-margin advance and recession respectively.

Period	Terrestrial ice-margins			Lacustrine ice-margins			Marine ice-margins		
	n	Mean change (m)	Mean annual change (m)	n	Mean change (m)	Mean annual change (m)	n	Mean change (m)	Mean annual change (m)
1987-1992	2469	5.8	1.2	353	-5.3	-1.1	22	96.3	19.3
1992-2000	3325	-1.4	-0.2	439	-13.0	-1.6	35	-250.6	-31.3
2000-2005	3325	-24.0	-4.8	414	-28.3	-5.7	35	-640.3	-69.7
2005-2010	3325	-15.3	-3.1	401	-32.2	-6.4	35	-197.6	-39.5
2010-2015	3325	-13.8	-2.8	374	-57.3	-11.5	35	-417.8	-83.6

[DOUBLE COLUMN WIDTH]

LMM 1 identified a significant negative correlation between rate of ice-margin change and epoch ($p < 0.001$), signifying increasing rates of ice-margin recession in south-west Greenland between 1987 and 2015, irrespective of margin type (Table 5). The model also identified significant differences between rates of change at lacustrine and marine margins ($p < 0.001$), and lacustrine and terrestrial margins ($p < 0.001$) (Table 5). Marine margins exhibited both the greatest mean rates of ice-margin recession and the greatest variability in frontal behaviour throughout the study period, with rates of advance and recession at several termini exceeding 100 m per year (Table 4, Figure 4a). The magnitude

and variability of changes at terrestrial and lacustrine margins were more comparable, although changes at lacustrine margins were less clustered around the median and typically more negative than their terrestrial counterparts (Table 4, Figure 4b). Notably, although rates of recession increased at both terrestrial and lacustrine ice-margins between 1987 and 2015, recession at lacustrine margins increasingly outpaced that of terrestrial margins throughout the survey period (Figure 5).

Table 5. LMM results. Significant relationships are highlighted in bold.

LMM No.	Ind. Variables	Estimate	Std. Error	t value	95 % Confidence intervals		p value
					lower	upper	
1	(Intercept)	-0.167	0.024	-6.975	-0.214	-0.120	< 0.001
	Epoch	-0.120	0.007	-17.360	-0.134	-0.107	< 0.001
	Type:Marine*	-2.637	0.088	-29.907	-2.809	-2.464	< 0.001
	Type:Terrestrial*	0.215	0.025	8.466	0.165	0.265	< 0.001
	Latitude	0.020	0.008	2.453	0.004	0.036	0.014
2(a)	(Intercept)	-0.039	0.040	-0.986	-0.117	0.039	0.324
	Latitude	0.065	0.026	2.438	0.013	0.116	0.015
	Altitude	0.132	0.025	5.241	0.083	0.181	< 0.001
	Area	-0.191	0.022	-8.687	-0.234	-0.148	< 0.001
	Epoch	-0.157	0.022	-7.215	-0.200	-0.114	< 0.001
	Persistence	0.030	0.103	0.293	-0.171	0.231	0.770
2(b)	(Intercept)	-0.072	0.040	-1.796	-0.150	0.006	0.073
	Latitude	0.068	0.026	2.576	0.016	0.119	0.010
	Altitude	0.132	0.025	5.299	0.084	0.181	< 0.001
	Intersect length	-0.223	0.022	-10.026	-0.267	-0.180	< 0.001
	Epoch	-0.153	0.022	-7.085	-0.196	-0.111	< 0.001
	Persistence	0.094	0.103	0.917	-0.107	0.295	0.359

* Note reference values for categorical variables 'Type' are lacustrine.

[DOUBLE COLUMN WIDTH]

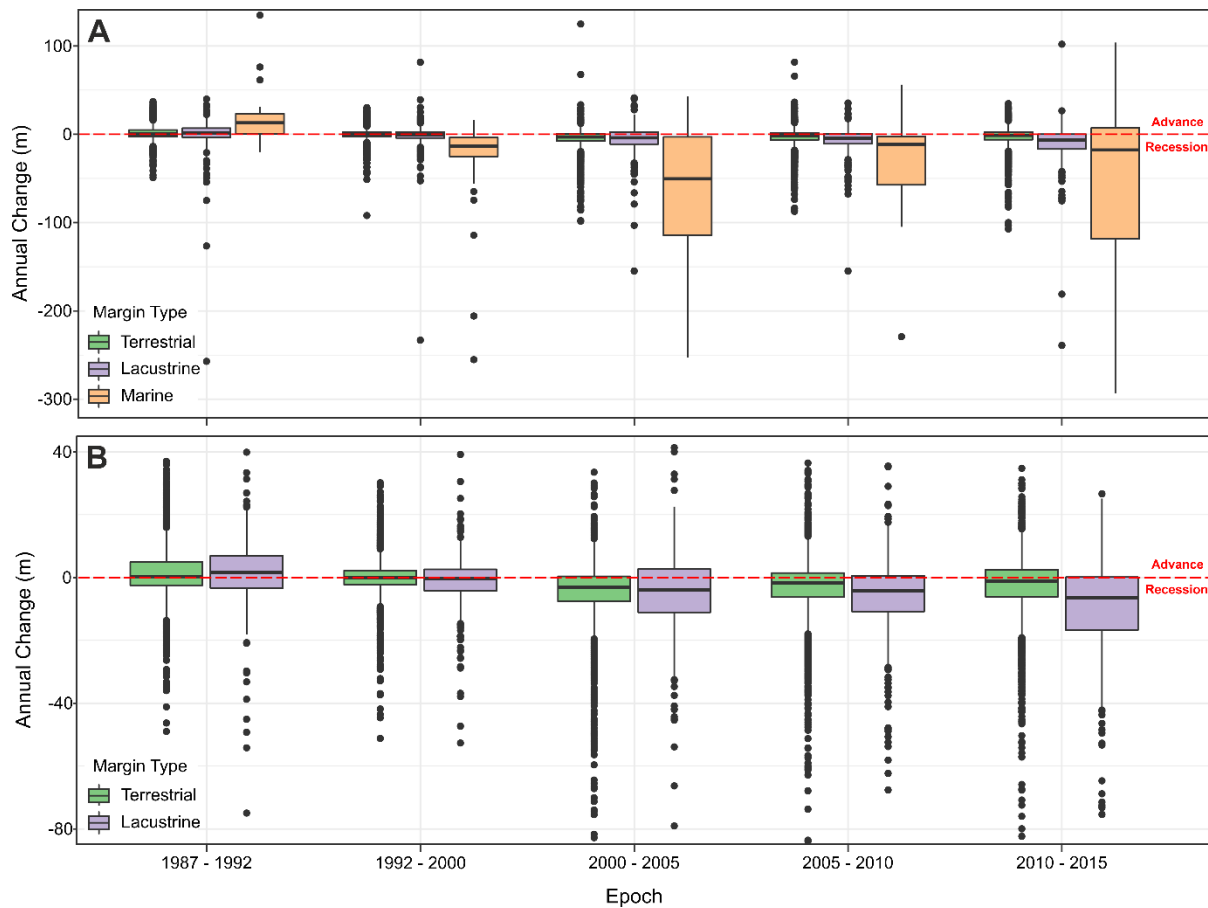


Figure 4. Box plots of ice-margin change throughout the study period at: (a) terrestrial, lacustrine and marine margins; and (b) terrestrial and lacustrine margins only. Note positive and negative values of annual change represent ice-margin advance and recession respectively. To improve clarity, 7 and 21 outlying data points have been cropped from panels (a) and (b) respectively.

[DOUBLE COLUMN WIDTH]

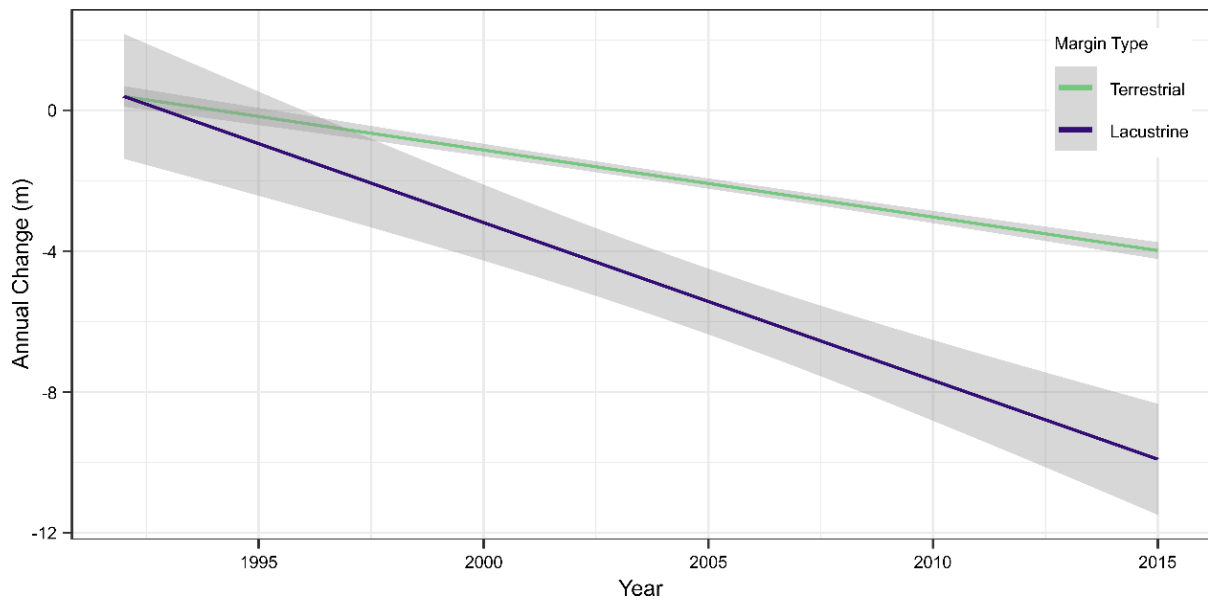


Figure 5. Linear regression of annual change and year, showing trends in ice-margin recession at terrestrial and lacustrine margins. The final year of each epoch has been used to plot the linear relationship. Grey shading represents the 95 % confidence interval. Individual data points have been removed to improve clarity (terrestrial $n = 15769$; lacustrine $n = 1981$).

[DOUBLE COLUMN WIDTH]

3.3 CONTROLS ON LACUSTRINE ICE-MARGIN CHANGE

Both variants of LMM 2 identified a number of significant relationships between lake parameters and rates of change at lacustrine margins (Table 5). The significant positive correlation between latitude and rate of change ($p < 0.05$) indicates that ice-margin recession was accentuated at lower latitudes (Figure 6a). Altitude was also found to act as a control on ice-margin change ($p < 0.001$), with increased rates of recession at lower altitudes (Figure 6b). Both lake area ($p < 0.001$) and intersect length ($p < 0.001$) possessed a similar significant negative correlation with rate of change, demonstrating that increased rates of ice-margin recession are associated with larger lakes and longer lake – ice-margin interfaces (Figures 6c, 6d). Finally, there was a significant negative correlation between epoch and rate of change ($p < 0.001$), signifying that rates of recession at lacustrine margins increased

throughout the duration of the study (Figure 6e). No significant correlation was found between persistence and rate of ice-margin change.

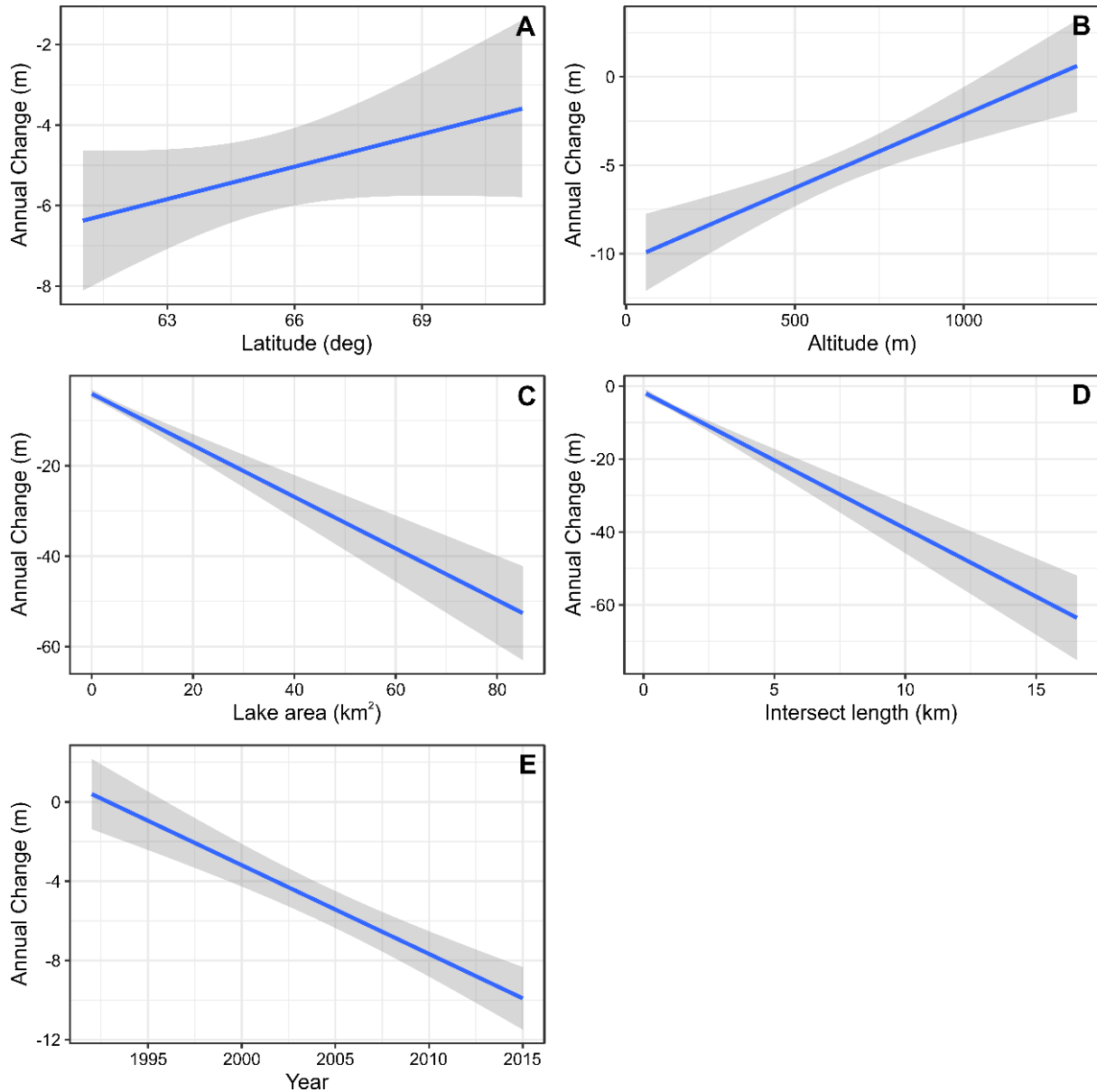


Figure 6. Linear regressions of annual change at lacustrine margins and lake parameters, comprising: (a) latitude; (b) altitude; (c) lake area; (d) intersect length; and (e) year. Note the final year of each epoch has been used to plot the linear relationship in (e). Grey shading represents the 95 % confidence interval. Individual data points have been removed to improve clarity (n = 1981).

[DOUBLE COLUMN WIDTH]

4. DISCUSSION

4.1 ICE-MARGIN CHANGE IN SOUTH-WEST GREENLAND

The temporal patterns of ice-margin advance and recession that we record in south-west Greenland broadly reflect previously-documented changes in ice sheet mass balance. Notably, in contrast to the mean ice-margin recession observed at all margin types post-1992, a mean advance at terrestrial and marine margins, and concurrent minima of lacustrine margin recession, is evident between 1987 and 1992 (Table 4). Although this distinction could be accentuated by the unavailability of satellite imagery from the southern reaches of the survey area in 1987 (Table 3), this pattern coincides with existing records of outlet glacier advance and general ice sheet expansion in the southern and western GrIS during the 1980s (e.g. Weidick, 1991; Zwally, 1989; Van Tatenhove et al., 1995; Knight et al., 2000) following a period of net mass gain in the preceding decade (Mouginot et al., 2019). Similarly, the period of ice-margin recession recorded post-1992 occurs following a transition to net mass loss at the GrIS in the 1980s (Mouginot et al., 2019), and is sustained through a further fivefold increase in the rate of mass loss between the 1990s and 2010 (Shepherd et al., 2020). However, the statistically significant differences between rates of change at the disparate margin types (Table 5) and considerable differences in variability of frontal behaviour (Figure 4) are indicative of heterogeneous responses at the respective terrestrial, lacustrine and marine margins of the GrIS, despite undergoing comparable climatic forcing over the survey duration.

The relative magnitude and variability of the changes recorded at the disparate ice-marginal environments in this study are similar to those observed at the western margins of the GrIS in the mid-20th century by Warren (1991), in which marine margins were found to exhibit the greatest magnitude and variability in frontal behaviour, and terrestrial margins the least. Because terrestrial termini lack oceanic or lacustrine forcing, changes in ice-margin extent are typically a delayed response to regional climatic forcing, with inter-glacier variability arising from glacier-specific factors, including: glacier geometry; hypsometry; debris-cover; and local climatic conditions (e.g. Pelto and Hedlund, 2001;

Scherler et al., 2011; Davies et al., 2012; Sakai and Fujita, 2017; Lovell et al., 2019). Consequently, the relatively limited variability in frontal behaviour at the terrestrial margins of the GrIS, in comparison to its marine margins, was expected (Figure 4a), and has been similarly observed in analyses of outlet glacier and PGIC extent in south-eastern Greenland over the same period (e.g. Mernild et al., 2012). Furthermore, the low magnitude of the changes observed at terrestrial margins compares favourably with existing records of terrestrial frontal behaviour in western Greenland in the 1990s and 2000s (e.g. Moon and Joughin, 2008; Carr et al., 2013).

In comparison to terrestrial margins, marine termini demonstrated considerably greater magnitude and variability in frontal behaviour over the duration of the study, with a mean annual advance of 19 m a^{-1} between 1987 and 1992, succeeded by mean annual recessions exceeding 31 m a^{-1} in all remaining periods (Table 4). In addition, the mean changes masked considerable complexity in the behaviour of individual marine terminating glaciers, with advances and recessions in the order of 10s and 100s of m a^{-1} respectively becoming increasingly prevalent from 2000-2005 onwards (Figure 4a). Isolating the exact drivers of change at marine ice-margins is challenging due to the complexities and interactions of both atmospheric and oceanic forcings, as well as glacier-specific controls including terminus geometry and bathymetry (McFadden et al., 2011; Porter et al., 2018). However, oceanic forcing is increasingly recognised as a key control on the dynamics of the marine outlets of the GrIS (Seale et al., 2011; Straneo and Heimbach, 2013). Accordingly, the observed transition from mean terminus advance to mean terminus recession at marine margins in 1992-2000 coincides with recorded increases in subsurface ocean temperatures along the west coast of Greenland in the mid-1990s (Myers et al., 2007; Holland et al., 2008), which are hypothesised to have triggered the collapse of several floating termini and a subsequent phase of regional marine ice-margin recession in response to debuttressing (e.g. Joughin et al., 2012). A further increase in marine ice-margin recession observed in this study in the early 2000s also concurs with similar observations from the same time period at

marine terminating outlets in south-eastern Greenland (Mernild et al., 2012) and across the wider ice sheet (Moon and Joughin, 2008; Howat and Eddy, 2011).

Despite mean changes in marine ice-margin extent being approximately an order of magnitude greater than those recorded at terrestrial and lacustrine ice-margins between 1987 and 2015, caution is necessary when interpreting and comparing the frontal behaviour of the disparate ice-marginal environments of the GrIS. In particular, marine ice-margins constitute by far the smallest component of the overall dataset ($n = 22-35$), and typically exhibit seasonal variations in terminus advance and recession that can be challenging to control for using multi-annual snapshots of terminus position (Schild and Hamilton, 2013). Furthermore, the relatively similar magnitudes of change observed at terrestrial and lacustrine termini conceal a notable divergence in the behaviour of the respective margin types over the duration of the study. In particular, the persistently negative values of mean changes at lacustrine margins, coupled with a progressive increase in their magnitude and their increased outpacing of change at terrestrial margins (Table 4, Figure 5), could be indicative of amplified lacustrine forcing and mass loss at the lake terminating margins of the GrIS between 1987 and 2015.

4.2 LACUSTRINE ICE-MARGIN RECESSION

The observed dissimilarities in the frontal behaviour of the terrestrial and lake terminating margins of the GrIS over the course of the study can be explained by the impact of lacustrine forcing on ice-margin dynamics. In particular, lake formation has significant implications for processes and rates of mass loss at ice-margins through the onset of both calving (Kirkbride, 1993; Motyka et al., 2003) and subaqueous melt (Eijpen et al., 2003; Haresign and Warren, 2005; Truffer and Motyka, 2016). Furthermore, ice-marginal lake formation can destabilise and perturb wider ice-margin dynamics through the initiation of a positive feedback whereby enhanced rates of mass loss increase local ice-surface gradients, thus promoting acceleration, thinning and fracture of the ice-margin, which in turn creates favourable

conditions for amplified calving losses (Benn et al., 2007; Carrivick and Tweed, 2013). This feedback has been invoked as the cause of the rapid ice-margin recession observed at an increasing number of alpine glaciers (Naruse and Skvarca, 2000; Boyce et al., 2007; Basnett et al., 2013; Trussel et al., 2013; King et al., 2018; Liu et al., 2020).

The correlations between rate of ice-margin change and lake area and intersect length respectively (Figure 6c-d, Table 5), suggest that lake size exerts a control on rates of mass loss at lacustrine margins. Although the augmented rates of ice-margin recession at larger lakes can be hypothesised to arise from the combined effects of calving and subaqueous melt occurring over a greater length of the ice-margin, it is likely that the greater water depths typically associated with larger lakes (e.g. Huggel et al., 2002; Cook and Quincey, 2015) are also a key driver of ice-margin recession. In particular, several empirical relationships have linked increased calving rates to greater lake depths (Warren et al., 1995; Warren and Kirkbride, 2003), and accelerated rates of lacustrine ice-margin recession have been observed following the retreat of termini into glacial overdeepenings (e.g. Kirkbride, 1993; Boyce et al., 2007; Larsen et al., 2015). In addition, the increased buoyancy and reduced effective pressure apparent at ice-margins terminating in deeper water favours the positive feedback between mass loss and terminus recession.

Increases in lake area and depth could also explain the progressive growth in mean annual lacustrine margin recession rates by an order of magnitude throughout the study, from 1.1 ma^{-1} between 1987 and 1992 to 11.5 ma^{-1} between 2010 and 2015 (Table 4, Figure 6e). A behavioural analysis of the lake dataset in Carrivick and Quincey (2014) revealed that ~45 % of all ice-marginal lakes in south-west Greenland formed or increased in size between 1987 and 2010, in contrast to only ~30 % of lakes decreasing in size or draining over the same period. Furthermore, the inverse bed slope along much of the ice sheet margin in south-west Greenland creates favourable conditions for ongoing lake expansion in response to ice-margin recession (Carrivick et al., 2017a; Morlighem et al., 2017). Lake

persistence was the only independent variable in the LMMs that did not significantly correlate with the rate of ice-margin change at lacustrine termini (Table 5), which may be indicative of a multifaceted relationship between ice-margin recession and lake stability. For example, although the most persistent lakes may be associated with greater rates of ice-margin recession due to their extended prevalence, lakes in contact with rapidly retreating ice-margins may also be inherently less stable due to increased opportunities for lake drainage through failure of the ice-dam or rapid changes to lake morphometry (e.g. Russell et al., 2011; Carrivick et al., 2017b; Carrivick and Tweed, 2019).

An additional cause of the enhanced rates of recession at lacustrine margins observed over the duration of this survey could be the lengthening of the season over which lacustrine processes, including subaqueous melt and calving, were able to promote mass loss. For example, analyses of non ice-contact lakes in the Arctic have identified an earlier break-up of winter ice-cover and an increase in ice-free days in response to atmospheric warming over recent decades (Duguay et al., 2006; Smejkalova et al., 2016; Surdu et al., 2016). Similar changes to the ice-cover regimes of ice-marginal lakes in south-west Greenland could therefore have amplified ice-margin recession through the prolonged operation of lacustrine processes associated with higher rates of mass loss, such as melt-undercutting (e.g. Mallalieu et al., 2020). These processes are likely to be further accentuated in lakes with a reduced duration of ice-cover by enhanced lake temperatures arising from the low albedo of open water. Notably, the mean annual lacustrine margin recession rates measured in this study increased following the switch to a negative phase of the North Atlantic Oscillation in the mid-1990s (Table 4), which is typically associated with enhanced summertime warming in west Greenland (Hanna et al., 2008; Bevis et al., 2019). In addition, further evidence of climatic control on rates of lacustrine margin recession is provided by the significant positive correlations between ice-margin change and latitude and altitude respectively (Figure 6a-b, Table 5), which highlight a strong association between high rates of lacustrine recession and the warmer climatic conditions typically associated with lower latitudes and altitudes. Consequently, the relationships identified here between latitude, altitude and

rates of lacustrine margin change, could be considered as tentative indicators of the future response of lacustrine margins to anticipated increases in atmospheric forcing in western Greenland (Bevis et al., 2019).

4.3 IMPLICATIONS AND FUTURE RESEARCH

In addition to enhancing local rates of ice-margin recession, the presence of lakes at the margin of the GrIS could have profound implications for wider ice sheet dynamics and stability. For example, Price et al. (2008) demonstrated that dynamic changes at the margins of the GrIS can propagate dozens of kilometres up-ice via longitudinal coupling. Therefore enhanced recession at lacustrine margins and resultant increases in surface gradients have significant potential to amplify surface velocities and promote dynamic thinning up-ice of the lacustrine termini, particularly where lakes are large and deep relative to the thickness of the ice-margin. Similar responses to lake formation and growth have been extensively documented in the Himalaya, where lacustrine terminating glaciers account for an increasingly disproportionate share of regional mass loss (Basnett et al., 2013; King et al., 2018; Brun et al., 2019; King et al., 2019). Currently 434 km (~9 %) of the ice sheet margin in south-west Greenland terminates in a lacustrine setting, in contrast to 153 km (~3 %) in a marine setting (Table 3). However, thinning at the margins of the ice-sheet (Krabill et al., 2004; Pritchard et al., 2009), coupled with continued atmospheric warming (Pattyn et al., 2018; Bevis et al., 2019) and the recession of the ice-margin over an inverse bed slope (Carrivick et al., 2017a; Morlighem et al., 2017), will create favourable conditions for enhanced ice-marginal lake formation and growth in south-west Greenland in coming decades. Additionally, over longer timescales, the recession of marine termini onto land (e.g. Joughin et al., 2010; Nick et al. 2013) will further increase the potential for lake formation at the ice sheet margin. Consequently, it can be hypothesised that ice-marginal lakes will play an increasingly important role in rates and patterns of deglaciation in Greenland, and that continued lake expansion will amplify future mass loss from the south-western margin of the GrIS. Furthermore, inadequate consideration of the impacts of lacustrine forcing at the margin of the GrIS could lead to increasing

error in projections of the ice sheet's response to climate change, and its contribution to sea level rise. The inclusion and parameterisation of lake – ice-margin interactions in numerical ice sheet models is therefore increasingly desirable (Carrivick et al., 2020).

A more advanced understanding of the impact of lacustrine forcing on the margin of the GrIS could be developed by focusing future research efforts in three main areas. Firstly, sections of the ice-margin susceptible to lake formation and growth could be determined through the development of morphometric and dynamic criteria, similar to those employed to forecast ice-marginal lake formation in the Himalaya (Reynolds, 2000; Quincey et al., 2007), particularly if integrated with recent high-resolution mapping of GrIS bed topography (e.g. Morlighem et al., 2017). In addition, knowledge of basal topography and ice thickness can facilitate predictions of lake area and depth, which are significant controls on rates of recession at lacustrine margins (Figure 6c). Secondly, regional-scale analyses of changes in velocity, structure and ice-surface elevation up-ice of the lacustrine termini of the GrIS are necessary to determine the magnitude of the dynamic response of the ice-sheet to lake formation and thus refine estimates of mass loss and sea level rise from lacustrine margins. This objective, and the extent to which the observations and conclusions drawn from this study in south-west Greenland may be applicable to the wider ice sheet, will be greatly facilitated by the recent generation of the first Greenland-wide multi-sensor inventory of ice-marginal lakes in How et al. (2021). Finally, local-scale analyses of lacustrine ice-margin dynamics are required to improve knowledge of the mechanisms driving enhanced ice-margin recession. In particular, calving processes and rates of subaqueous melt remain relatively poorly constrained at lacustrine ice-margins (Haresign and Warren, 2005; Trussel et al., 2013; Purdie et al., 2016; Truffer and Motyka, 2016; Mallalieu et al., 2020).

5. CONCLUSIONS

This study has presented the first systematic analysis of changes in the extent of the terrestrial, lacustrine and marine margins of the GrIS in south-west Greenland between 1987 and 2015. The analysis revealed an extended and accelerating phase of ice-margin recession in south-west Greenland from 1992 onwards, irrespective of ice-margin type. However, significant differences in rates of ice-margin change also indicated a heterogeneous response at the respective ice-marginal environments of the GrIS to comparable climatic forcing over the survey duration. Marine terminating ice-margins exhibited the greatest magnitude and variability in ice-margin change, with rapid ice-margin recession becoming pervasive from 1992. Mean ice-margin recession rates and variability in frontal behaviour were also consistently greater at lacustrine termini than their terrestrial counterparts. In addition, mean ice-margin recession rates at lacustrine termini increased by an order of magnitude over the duration of the survey and progressively outpaced those measured at terrestrial ice-margins. This study has also identified significant correlations between rates of lacustrine ice-margin recession and lake parameters, including lake area, latitude, altitude and the length of the lake – ice-margin interface. The progressive increase in rates of lacustrine ice-margin recession measured over the duration of the survey are theorised to have arisen from increases in lake size and a lengthening of the season in which calving and subaqueous melt processes can promote mass loss at lacustrine termini. These results suggest that ice-marginal lakes have become increasingly significant drivers of ice-margin recession and thus mass loss at the GrIS, and are likely to further increase in importance in response to enhanced ice-marginal lake prevalence in coming decades. Further research is therefore necessary to better parameterise the causal connections between ice-marginal lake evolution and enhanced ice-margin recession in Greenland, and thus refine the contribution of mass loss from the lacustrine margins of the GrIS to sea level rise projections.

ACKNOWLEDGEMENTS

JM was funded by a Graduate Assistantship from the School of Geography at the University of Leeds. CR was the recipient of a NERC Case Award (grant ref. NE/K007599/1). The authors would like to thank

two anonymous reviewers for their valuable comments and insights which helped to enhance this manuscript.

DATA STATEMENT

The dataset of ice-margin change used in this analysis is available from the UK Polar Data Centre: <https://doi.org/...> The R code for the statistical analyses is available from GitHub: <https://doi.org/...> (DOIs will be confirmed prior to publication).

REFERENCES

- Aschwanden, A., Fahnestock, M.A., Truffer, M., Brinkerhoff, D.J., Hock, R., Khroulev, C., Mottram, R. and Khan, S.A. 2019. Contribution of the Greenland Ice Sheet to sea level over the next millennium. *Science Advances*. **5**(6), eaav9396.
- Basnett, S., Kulkarni, A.V. and Bolch, T. 2013. The influence of debris cover and glacial lakes on the recession of glaciers in Sikkim Himalaya, India. *Journal of Glaciology*. **59**(218), pp.1035-1046.
- Bates, D., Machler, M., Bolker, B.M. and Walker, S.C. 2015. Fitting Linear Mixed-Effects Models Using lme4. *Journal of Statistical Software*. **67**(1), pp.1-48.
- Benn, D.I., Warren, C.R. and Mottram, R.H. 2007. Calving processes and the dynamics of calving glaciers. *Earth-Science Reviews*. **82**(3-4), pp.143-179.
- Bevan, S.L., Luckman, A.J. and Murray, T. 2012. Glacier dynamics over the last quarter of a century at Helheim, Kangerdlugssuaq and 14 other major Greenland outlet glaciers. *The Cryosphere*. **6**(5), pp.923-937.
- Bevis, M., Harig, C., Khan, S.A., Brown, A., Simons, F.J., Willis, M., Fettweis, X., van den Broeke, M.R., Madsen, F.B., Kendrick, E., Caccamise, D.J., van Dam, T., Knudsen, P. and Nylén, T. 2019. Accelerating changes in ice mass within Greenland, and the ice sheet's sensitivity to atmospheric forcing. *Proceedings of the National Academy of Sciences*. **116**(6), pp.1934-1939.
- Bjørk, A.A., Aagaard, S., Lutt, A., Khan, S.A., Box, J.E., Kjeldsen, K.K., Larsen, N.K., Korsgaard, N.J., Cappelen, J., Colgan, W.T., Machguth, H., Andresen, C.S., Peings, Y. and Kjaer, K.H. 2018. Changes in Greenland's peripheral glaciers linked to the North Atlantic Oscillation. *Nature Climate Change*. **8**(1), pp.48-52.
- Bjørk, A.A., Kjaer, K.H., Korsgaard, N.J., Khan, S.A., Kjeldsen, K.K., Andresen, C.S., Box, J.E., Larsen, N.K. and Funder, S. 2012. An aerial view of 80 years of climate-related glacier fluctuations in southeast Greenland. *Nature Geoscience*. **5**(6), pp.427-432.
- Boyce, E.S., Motyka, R.J. and Truffer, M. 2007. Flotation and retreat of a lake-calving terminus, Mendenhall Glacier, Southeast Alaska, USA. *Journal of Glaciology*. **53**(181), pp.211-224.
- Brun, F., Wagnon, P., Berthier, E., Jomelli, V., Maharjan, S.B., Shrestha, F. and Kraaijenbrink, P.D.A. 2019. Heterogeneous Influence of Glacier Morphology on the Mass Balance Variability in High Mountain Asia. *Journal of Geophysical Research: Earth Surface*. **124**(6), pp.1331-1345.

613 Carr, J.R., Stokes, C.R. and Vieli, A. 2013. Recent progress in understanding marine-terminating Arctic
614 outlet glacier response to climatic and oceanic forcing: Twenty years of rapid change. *Progress in*
615 *Physical Geography: Earth and Environment*. **37**(4), pp.436-467.

616 Carrivick, J.L. and Quincey, D.J. 2014. Progressive increase in number and volume of ice-marginal lakes
617 on the western margin of the Greenland Ice Sheet. *Global and Planetary Change*. **116**, pp.156-163.

618 Carrivick, J.L. and Tweed, F.S. 2013. Proglacial lakes: character, behaviour and geological importance.
619 *Quaternary Science Reviews*. **78**, pp.34-52.

620 Carrivick, J.L. and Tweed, F.S. 2019. A review of glacier outburst floods in Iceland and Greenland with
621 a megafloods perspective. *Earth-Science Reviews*. **196**, 102876.

622 Carrivick, J.L., Tweed, F.S., Ng, F., Quincey, D.J., Mallalieu, J., Ingeman-Nielsen, T., Mikkelsen, A.B.,
623 Palmer, S.J., Yde, J.C., Homer, R. and Russell, A.J. 2017b. Ice-dammed lake drainage evolution at Russell
624 Glacier, West Greenland. *Frontiers in Earth Science*. **5**, 2017.00100

625 Carrivick, J.L., Tweed, F.S., Sutherland, J.L. and Mallalieu, J. 2020. Toward numerical modeling of
626 interactions between ice-marginal proglacial lakes and glaciers. *Frontiers in Earth Science*. **8**,
627 2020.577068.

628 Carrivick, J.L., Yde, J., Russell, A.J., Quincey, D.J., Ingeman-Nielsen, T. and Mallalieu, J. 2017a. Ice-
629 margin and meltwater dynamics during the mid-Holocene in the Kangerlussuaq area of west
630 Greenland. *Boreas*. **46**(3), pp.369-387.

631 Catania, G.A., Stearns, L.A., Sutherland, D.A., Fried, M.J., Bartholomaeus, T.C., Morlighem, M., Shroyer,
632 E. and Nash, J. 2018. Geometric Controls on Tidewater Glacier Retreat in Central Western Greenland.
633 *Journal of Geophysical Research-Earth Surface*. **123**(8), pp.2024-2038.

634 Citterio, M., Paul, F., Ahlstrom, A.P., Jepsen, H.F. and Weidick, A. 2009. Remote sensing of glacier
635 change in West Greenland: accounting for the occurrence of surge-type glaciers. *Annals of Glaciology*.
636 **50**(53), pp.70-80.

637 Cook, S.J. and Quincey, D.J. 2015. Estimating the volume of Alpine glacial lakes. *Earth Surface*.
638 *Dynamics*. **3**, pp.559-575.

639 Davies, B.J., Carrivick, J.L., Glasser, N.F., Hambrey, M.J. and Smellie, J.L. 2012. Variable glacier response
640 to atmospheric warming, northern Antarctic Peninsula, 1988–2009. *The Cryosphere*. **6**(5), pp.1031-
641 1048.

642 Ding Q., Wallace J.M., Battisti D.S., Steig E.J., Gallant A.J.E., Kim H. and Geng, L. 2014. Tropical forcing
643 of the recent rapid Arctic warming in northeastern Canada and Greenland. *Nature*. **509**, pp.209-212.

644 Dormann, C.F., Elith, J., Bacher, S., Buchmann, C., Carl, G., Carre, G., Marquez, J.R.G., Gruber, B.,
645 Lafourcade, B., Leitao, P.J., Munkemuller, T., McClean, C., Osborne, P.E., Reineking, B., Schroder, B.,
646 Skidmore, A.K., Zurell, D. and Lautenbach, S. 2013. Collinearity: a review of methods to deal with it
647 and a simulation study evaluating their performance. *Ecography*. **36**(1), pp.27-46.

648 Duguay, C.R., Prowse, T.D., Bonsal, B.R., Brown, R.D., Lacroix, M.P. and Menard, P. 2006. Recent trends
649 in Canadian lake ice cover. *Hydrological Processes*. **20**(4), pp.781-801.

650 Eijpen, K.J., Warren, C.R. and Benn, D.I. 2003. Subaqueous melt rates at calving termini: a laboratory
651 approach. *Annals of Glaciology*. **36**(1), pp.179-183.

652 Hall, D.K., Riggs, G.A. and Salomonson, V.V. 1995. Development of methods for mapping global snow
653 cover using moderate resolution imaging spectroradiometer data. *Remote Sensing of Environment*.
654 **54**(2), pp.127-140.

655 Hanna, E., Huybrechts, P., Steffen, K., Cappelen, J., Huff, R., Shuman, C., Irvine-Fynn, T., Wise, S. and
656 Griffiths, M. 2008. Increased runoff from melt from the Greenland Ice Sheet: A response to global
657 warming. *Journal of Climate*. **21**(2), pp.331-341.

658 Hanna, E., Navarro, F.J., Pattyn, F., Domingues, C.M., Fettweis, X., Ivins, E.R., Nicholls, R.J., Ritz, C.,
659 Smith, B., Tulaczyk, S., Whitehouse, P.L. and Zwally, H.J. 2013. Ice-sheet mass balance and climate
660 change. *Nature*. **498**(7452), pp.51-59.

661 Haresign, E. and Warren, C.R. 2005. Melt rates at calving termini: a study at Glaciar León, Chilean
662 Patagonia. *Geological Society, London, Special Publications*. **242**(1), pp.99-109.

663 Hill, E.A., Carr, J.R., Stokes, C.R. and Gudmundsson, G.H. 2018. Dynamic changes in outlet glaciers in
664 northern Greenland from 1948 to 2015. *The Cryosphere*. **12**(10), pp.3243-3263.

665 Holland, D.M., Thomas, R.H., de Young, B., Ribergaard, M.H. and Lyberth, B. 2008. Acceleration of
666 Jakobshavn Isbræ triggered by warm subsurface ocean waters. *Nature Geoscience*. **1**(10), pp.659-664.

667 How, P., Messerli, A., Mätzler, E., Santoro, M., Wiesmann, A., Caduff, R., Langley, K., Bojesen, M.H.,
668 Paul, F., Kääb, A. and Carrivick, J.L. 2021. Greenland-wide inventory of ice marginal lakes using a multi-
669 method approach. *Scientific Reports*. **11**, 4481.

670 Howat, I.M. and Eddy, A. 2011. Multi-decadal retreat of Greenland's marine-terminating glaciers.
671 *Journal of Glaciology*. **57**(203), pp.389-396.

672 Howat, I.M., Joughin, I., Fahnestock, M., Smith, B.E. and Scambos, T.A. 2008. Synchronous retreat and
673 acceleration of southeast Greenland outlet glaciers 2000-06: ice dynamics and coupling to climate.
674 *Journal of Glaciology*. **54**(187), pp.646-660.

675 Huggel, C., Kaab, A., Haeberli, W., Teyssere, P. and Paul, F. 2002. Remote sensing based assessment
676 of hazards from glacier lake outbursts: a case study in the Swiss Alps. *Canadian Geotechnical Journal*.
677 **39**(2), pp.316-330.

678 Joughin, I., Smith, B.E., Howat, I.M., Floricioiu, D., Alley, R.B., Truffer, M. and Fahnestock, M. 2012.
679 Seasonal to decadal scale variations in the surface velocity of Jakobshavn Isbrae, Greenland:
680 Observation and model-based analysis. *Journal of Geophysical Research: Earth Surface*. **117**, F02030.

681 Joughin, I., Smith, B.E., Howat, I.M., Scambos, T. and Moon, T. 2010. Greenland flow variability from
682 ice-sheet-wide velocity mapping. *Journal of Glaciology*. **56**, pp.415-430.

683 Kargel, J.S., Ahlstrøm, A.P., Alley, R.B., Bamber, J.L., Benham, T.J., Box, J.E., Chen, C., Christoffersen, P.,
684 Citterio, M., Cogley, J.G., Jiskoot, H., Leonard, G.J., Morin, P., Scambos, T., Sheldon, T. and Willis, I.
685 2012. Brief communication: Greenland's shrinking ice cover: "Fast times" but not that fast. *Cryosphere*.
686 **6**(3), pp.533-537.

687 King, O., Bhattacharya, A., Bhambri, R. and Bolch, T. 2019. Glacial lakes exacerbate Himalayan glacier
688 mass loss. *Scientific Reports*. **9**, 18145.

689 King, O., Dehecq, A., Quincey, D. and Carrivick, J. 2018. Contrasting geometric and dynamic evolution
690 of lake and land-terminating glaciers in the central Himalaya. *Global and Planetary Change*. **167**,
691 pp.46-60.

692 Kirkbride, M.P. 1993. The temporal significance of transitions from melting to calving termini at
693 glaciers in the central Southern Alps of New Zealand. *The Holocene*. **3**(3), pp.232-240.

694 Knight, P.G., Waller, R.I., Patterson, C.J., Jones, A.P. and Robinson, Z.P. 2000. Glacier advance, ice-
695 marginal lakes and routing of meltwater and sediment: Russell Glacier, Greenland. *Journal of*
696 *Glaciology*. **46**(154), pp.423-426.

697 Korsgaard, N.J., Nuth, C., Khan, S.A., Kjeldsen, K.K., Bjørk, A.A., Schomacker, A. and Kjær, K.H. 2016.
698 Digital elevation model and orthophotographs of Greenland based on aerial photographs from 1978–
699 1987. *Scientific Data*. **3**(1), 160032.

700 Krabill, W., Hanna, E., Huybrechts, P., Abdalati, W., Cappelen, J., Csatho, B., Frederick, E., Manizade,
701 S., Martin, C., Sonntag, J., Swift, R., Thomas, R. and Yungel, J. 2004. Greenland Ice Sheet: Increased
702 coastal thinning. *Geophysical Research Letters*. **31**(24) L24402.

703 Larsen, C.F., Burgess, E., Arendt, A.A., O'Neel, S., Johnson, A.J. and Kienholz, C. 2015. Surface melt
704 dominates Alaska glacier mass balance. *Geophysical Research Letters*. **42**(14), pp.5902-5908.

705 Lea, J.M., Mair, D.W.F. and Rea, B.R. 2014. Evaluation of existing and new methods of tracking glacier
706 terminus change. *Journal of Glaciology*. **60**(220), pp.323-332.

707 Leclercq, P.W., Weidick, A., Paul, F., Bolch, T., Citterio, M. and Oerlemans, J. 2012. Brief
708 communication "Historical glacier length changes in West Greenland". *Cryosphere*. **6**(6), pp.1339-
709 1343.

710 Liu Q., Mayer C., Wang X., Nie Y., Wu K., Wei J. and Liu S. 2020. Interannual flow dynamics driven by
711 frontal retreat of a lake-terminating glacier in the Chinese Central Himalaya. *Earth and Planetary
712 Science Letters*. **546**, 116450.

713 Lovell, A.M., Carr, J.R. and Stokes, C.R. 2019. Spatially Variable Glacier Changes in the Annapurna
714 Conservation Area, Nepal, 2000 to 2016. *Remote Sensing*. **11**(12), 1452.

715 Mallalieu, J., Carrivick, J.L., Quincey, D.J., Smith, M.W. and James, W.H., 2017. An integrated Structure-
716 from-Motion and time-lapse technique for quantifying ice-margin dynamics. *Journal of Glaciology*.
717 **63**(242), pp.937-949.

718 Mallalieu, J., Carrivick, J.L., Quincey, D.J. and Smith, M.W. 2020. Calving Seasonality Associated With
719 Melt-Undercutting and Lake Ice Cover. *Geophysical Research Letters*. **47**(8), GL086561.

720 McFadden, E.M., Howat, I.M., Joughin, I., Smith, B.E. and Ahn, Y. 2011. Changes in the dynamics of
721 marine terminating outlet glaciers in west Greenland (2000–2009). *Journal of Geophysical Research:*
722 *Earth Surface*. **116**, F02022.

723 McFeeters, S.K. 1996. The use of the Normalized Difference Water Index (NDWI) in the delineation of
724 open water features. *International Journal of Remote Sensing*. **17**(7), pp.1425-1432.

725 Mernild, S.H., Malmros, J.K., Yde, J.C. and Knudsen, N.T. 2012. Multi-decadal marine- and land-
726 terminating glacier recession in the Ammassalik region, southeast Greenland. *Cryosphere*. **6**(3),
727 pp.625-639.

728 Moon, T. and Joughin, I. 2008. Changes in ice front position on Greenland's outlet glaciers from 1992
729 to 2007. *Journal of Geophysical Research-Earth Surface*. **113**, F02022.

730 Morlighem, M., Williams, C.N., Rignot, E., An, L., Arndt, J.E., Bamber, J.L., Catania, G., Chauché, N.,
731 Dowdeswell, J.A., Dorschel, B., Fenty, I., Hogan, K., Howat, I., Hubbard, A., Jakobsson, M., Jordan, T.M.,
732 Kjeldsen, K.K., Millan, R., Mayer, L., Mouginot, J., Noël, B.P.Y., O'Cofaigh, C., Palmer, S., Rysgaard, S.,
733 Seroussi, H., Siegert, M.J., Slabon, P., Straneo, F., van den Broeke, M.R., Weinrebe, W., Wood, M. and
734 Zinglensen, K.B. 2017. BedMachine v3: Complete Bed Topography and Ocean Bathymetry Mapping of
735 Greenland From Multibeam Echo Sounding Combined With Mass Conservation. *Geophysical Research
736 Letters*. **44**(21), pp.11051-11061.

737 Motyka, R.J., O'Neel, S., Connor, C.L. and Echelmeyer, K.A. 2003. Twentieth century thinning of
738 Mendenhall Glacier, Alaska, and its relationship to climate, lake calving, and glacier run-off. *Global and
739 Planetary Change*. **35**(1-2), pp.93-112.

740 Mouginot, J., Rignot, E., Bjørk, A.A., van den Broeke, M., Millan, R., Morlighem, M., Noël, B., Scheuchl,
741 B. and Wood, M. 2019. Forty-six years of Greenland Ice Sheet mass balance from 1972 to 2018.
742 *Proceedings of the National Academy of Sciences*. **116**(19), pp.9239-9244.

743 Myers, P.G., Kulan, N. and Ribergaard, M.H. 2007. Irminger Water variability in the West Greenland
744 Current. *Geophysical Research Letters*. **34**(17), L17601.

745 Nick, F.M., Vieli, A., Andersen, M.L., Joughin, I., Payne, A., Edwards, T.L., Pattyn, F. and van de Wal,
746 R.S.W. 2013. Future sea-level rise from Greenland's main outlet glaciers in a warming climate. *Nature*.
747 **497**, pp.235-238.

748 Naruse, R. and Skvarca, P. 2000. Dynamic features of thinning and retreating Glaciar Upsala, a
749 Lacustrine Calving Glacier in southern Patagonia. *Arctic Antarctic and Alpine Research*. **32**(4), pp.485-
750 491.

751 Pattyn, F., Ritz, C., Hanna, E., Asay-Davis, X., DeConto, R., Durand, G., Favier, L., Fettweis, X., Goelzer,
752 H., Golledge, N.R., Kuipers Munneke, P., Lenaerts, J.T.M., Nowicki, S., Payne, A.J., Robinson, A.,
753 Seroussi, H., Trusel, L.D. and van den Broeke, M. 2018. The Greenland and Antarctic ice sheets under
754 1.5 °C global warming. *Nature Climate Change*. **8**(12), pp.1053-1061.

755 Pelto, M.S. and Hedlund, C. 2001. Terminus behavior and response time of North Cascade glaciers,
756 Washington, U.S.A. *Journal of Glaciology*. **47**(158), pp.497-506.

757 Porter, D.F., Tinto, K.J., Boghosian, A.L., Csatho, B.M., Bell, R.E. and Cochran, J.R. 2018. Identifying
758 Spatial Variability in Greenland's Outlet Glacier Response to Ocean Heat. *Frontiers in Earth Science*.
759 **6**(90), 2018.00090.

760 Price, S.F., Payne, A.J., Catania, G.A. and Neumann, T.A. 2008. Seasonal acceleration of inland ice via
761 longitudinal coupling to marginal ice. *Journal of Glaciology*. **54**(185), pp.213-219.

762 Pritchard, H.D., Arthern, R.J., Vaughan, D.G. and Edwards, L.A. 2009. Extensive dynamic thinning on
763 the margins of the Greenland and Antarctic ice sheets. *Nature*. **461**(7266), pp.971-975.

764 Purdie H., Bealing P., Tidey E., Gomez C. and Harrison J. 2016. Bathymetric evolution of Tasman Glacier
765 terminal lake, New Zealand, as determined by remote surveying techniques. *Global and Planetary*
766 *Change*. **147**, pp.1-11.

767 Quincey, D.J., Richardson, S.D., Luckman, A., Lucas, R.M., Reynolds, J.M., Hambrey, M.J. and Glasser,
768 N.F. 2007. Early recognition of glacial lake hazards in the Himalaya using remote sensing datasets.
769 *Global and Planetary Change*. **56**(1), pp.137-152.

770 Rastner, P., Bolch, T., Molg, N., Machguth, H., Le Bris, R. and Paul, F. 2012. The first complete inventory
771 of the local glaciers and ice caps on Greenland. *Cryosphere*. **6**(6), pp.1483-1495.

772 Reynolds, J.M. 2000. On the formation of supraglacial lakes on debris-covered glaciers. In: Nakawo,
773 M., et al. eds. *Debris-Covered Glaciers*. Wallingford: Int Assoc Hydrological Sciences, pp.153-161.

774 Roy, D.P., Wulder, M.A., Loveland, T.R., C.E. W., Allen, R.G., Anderson, M.C., Helder, D., Irons, J.R.,
775 Johnson, D.M., Kennedy, R., Scambos, T.A., Schaaf, C.B., Schott, J.R., Sheng, Y., Vermote, E.F., Belward,
776 A.S., Bindaschadler, R., Cohen, W.B., Gao, F., Hipple, J.D., Hostert, P., Huntington, J., Justice, C.O., Kilic,
777 A., Kovalsky, V., Lee, Z.P., Lymburner, L., Masek, J.G., McCorkel, J., Shuai, Y., Trezza, R., Vogelmann,
778 J., Wynne, R.H. and Zhu, Z. 2014. Landsat-8: Science and product vision for terrestrial global change
779 research. *Remote Sensing of Environment*. **145**, pp.154-172.

780 Russell, A.J., Carrivick, J.L., Ingeman-Nielsen, T., Yde, J.C. and Williams, M. 2011. A new cycle of
781 jökulhlaups at Russell Glacier, Kangerlussuaq, West Greenland. *Journal of Glaciology*. **57**(202), pp.238-
782 246.

783 Sakai, A. and Fujita, K. 2017. Contrasting glacier responses to recent climate change in high-mountain
784 Asia. *Scientific Reports*. **7**(1), 13717.

785 Scherler, D., Bookhagen, B. and Strecker, M.R. 2011. Spatially variable response of Himalayan glaciers
786 to climate change affected by debris cover. *Nature Geoscience*. **4**(3), pp.156-159.

787 Schild, K.M. and Hamilton, G.S. 2013. Seasonal variations of outlet glacier terminus position in
788 Greenland. *Journal of Glaciology*. **59**(216), pp.759-770.

789 Schomacker, A. 2010. Expansion of ice-marginal lakes at the Vatnajökull ice cap, Iceland, from 1999 to
790 2009. *Geomorphology*. **119**(3-4), pp.232-236.

791 Seale, A., Christoffersen, P., Mugford, R.I. and O'Leary, M. 2011. Ocean forcing of the Greenland Ice
792 Sheet: Calving fronts and patterns of retreat identified by automatic satellite monitoring of eastern
793 outlet glaciers. *Journal of Geophysical Research-Earth Surface*. **116**, F03013.

794 Shepherd, A., Ivins, E., Rignot, E., Smith, B., van den Broeke, M., Velicogna, I., Whitehouse, P., Briggs,
795 K., Joughin, I., Krinner, G., Nowicki, S., Payne, T., Scambos, T., Schlegel, N., Geruo, A., Agosta, C.,
796 Ahlstrøm, A., Babonis, G., Barletta, V.R., Bjørk, A.A., Blazquez, A., Bonin, J., Colgan, W., Csatho, B.,
797 Cullather, R., Engdahl, M.E., Felikson, D., Fettweis, X., Forsberg, R., Hogg, A.E., Gallee, H., Gardner, A.,
798 Gilbert, L., Gourmelen, N., Groh, A., Gunter, B., Hanna, E., Harig, C., Helm, V., Horvath, A., Horwath,
799 M., Khan, S., Kjeldsen, K.K., Konrad, H., Langen, P.L., Lecavalier, B., Loomis, B., Luthcke, S., McMillan,
800 M., Melini, D., Mernild, S., Mohajerani, Y., Moore, P., Mottram, R., Mouginot, J., Moyano, G., Muir, A.,
801 Nagler, T., Nield, G., Nilsson, J., Noël, B., Otosaka, I., Pattie, M.E., Peltier, W.R., Pie, N., Rietbroek, R.,
802 Rott, H., Sørensen, L.S., Sasgen, I., Save, H., Scheuchl, B., Schrama, E., Schröder, L., Seo, K.-W.,
803 Simonsen, S.B., Slater, T., Spada, G., Sutterley, T., Talpe, M., Tarasov, L., Jan van de Berg, W., van der
804 Wal, W., van Wessem, M., Vishwakarma, B.D., Wiese, D., Wilton, D., Wagner, T., Wouters, B., Wuite,
805 J. and The Imbie Team. 2020. Mass balance of the Greenland Ice Sheet from 1992 to 2018. *Nature*.
806 **579**, pp.233-239.

807 Smejkalova, T., Edwards, M.E. and Dash, J. 2016. Arctic lakes show strong decadal trend in earlier
808 spring ice-out. *Scientific Reports*. **6**, 38449.

809 Straneo, F. and Heimbach, P. 2013. North Atlantic warming and the retreat of Greenland's outlet
810 glaciers. *Nature*. **504**(7478), pp.36-43.

811 Surdu, C.M., Duguay, C.R. and Prieto, D.F. 2016. Evidence of recent changes in the ice regime of lakes
812 in the Canadian High Arctic from spaceborne satellite observations. *Cryosphere*. **10**(3), pp.941-960.

813 Sutherland, J.L., Carrivick, J.L., Gandy, N., Shulmeister, J., Quincey, D.J. and Cornford, S.L. 2020.
814 Proglacial lakes control glacier geometry and behavior during recession. *Geophysical Research Letters*.
815 **47**(19), GL088865.

816 Truffer, M. and Motyka, R.J. 2016. Where glaciers meet water: Subaqueous melt and its relevance to
817 glaciers in various settings. *Reviews of Geophysics*. **54**, pp.220-239.

818 Trusel, L.D., Das, S.B., Osman, M.B., Evans, M.J., Smith, B.E., Fettweis, X., McConnell, J.R., Noël, B.P.Y.
819 and van den Broeke, M.R. 2018. Nonlinear rise in Greenland runoff in response to post-industrial Arctic
820 warming. *Nature*. **564**(7734), pp.104-108.

821 Trussel, B.L., Motyka, R.J., Truffer, M. and Larsen, C.F. 2013. Rapid thinning of lake-calving Yakutat
822 Glacier and the collapse of the Yakutat Icefield, southeast Alaska, USA. *Journal of Glaciology*. **59**(213),
823 pp.149-161.

824 Tsutaki S., Fujita K., Nuimura T., Sakai A., Sugiyama S., Komori J. and Tshering P. 2019. Contrasting
825 thinning patterns between lake- and land-terminating glaciers in the Bhutanese Himalaya. *The*
826 *Cryosphere*. **13**, pp. 2733-2750.

827 Van Tatenhove, F.G.M., Roelfsema, C.M., Blommers, G. and Voorden, A.V. 1995. Change in position
828 and altitude of a small outlet glacier during the period 1943–92: Leverett Glacier, West Greenland.
829 *Annals of Glaciology*. **21**, pp.251-258.

- 830 Warren, C.R. 1991. Terminal environment, topographic control and fluctuations of West Greenland
831 glaciers. *Boreas*. **20**(1), pp.1-15.
- 832 Warren, C.R., Greene, D.R. and Glasser, N.F. 1995. Glaciar Upsala, Patagonia: Rapid calving retreat in
833 fresh water. *Annals of Glaciology*. **21**, pp.311-316.
- 834 Warren, C.R. and Kirkbride, M.P. 2003. Calving speed and climatic sensitivity of New Zealand lake-
835 calving glaciers. *Annals of Glaciology*. **36**, pp.173-178.
- 836 Weidick, A. 1991. Present-day expansion of the southern part of the Inland Ice. *Rapport Gronlands*
837 *Geologiske Undersogelse*. **152**, pp.73-79.
- 838 Zwally, H.J. 1989. Growth of Greenland ice sheet - Interpretation. *Science*. **246**(4937), pp.1589-1591.
839